On optimal interpolation schemes for particle tracking in turbulence

EINDHOVEN UNIVERSITY OF TECHNOLOGY
Department of Mathematics and Computer Science

CASA-Report 12-40
November 2012

On optimal interpolation schemes for particle tracking in turbulence

by

M.A.T. van Hinsberg, J.H.M. ten Thije Boonkkamp, F. Toschi, H.J.H. Clercx

Centre for Analysis, Scientific computing and Applications
Department of Mathematics and Computer Science
Eindhoven University of Technology
P.O. Box 513
5600 MB Eindhoven, The Netherlands
ISSN: 0926-4507

On optimal interpolation schemes for particle tracking in turbulence

M.A.T. van Hinsberg,[1,*] J.H.M. ten Thije Boonkkamp,[2] F. Toschi,[1,2,3] and H.J.H. Clercx[1,4,†]

[1] *Department of Physics, Eindhoven University of Technology, PO Box 513, 5600MB Eindhoven, The Netherlands,*
[2] *Department of Mathematics and Computer Science, Eindhoven University of Technology, PO Box 513, 5600MB Eindhoven, The Netherlands,*
[3] *CNR, Istituto per le Applicazioni del Calcolo, Via dei Taurini 19, 00185 Rome, Italy,*
[4] *Department of Applied Mathematics, University of Twente, PO Box 217, 7500 AE Enschede, The Netherlands,*

An important aspect in numerical simulations of particle-laden turbulent flows is the interpolation of the flow field needed for the computation of the Lagrangian trajectories. The accuracy of the interpolation method has direct consequences for the acceleration spectrum of the fluid particles and is therefore also important for the correct evaluation of the hydrodynamic forces for almost neutrally buoyant particles, common in many environmental applications. In order to systematically choose the optimal tradeoff between interpolation accuracy and computational cost we focuss on comparing errors: the interpolation error is compared with the discretisation error of the flow field. In this way one can prevent unnecessary computations and still retain the accuracy of the turbulent flow simulation. From the analysis a practical method is proposed that enables direct estimation of the interpolation and discretization error from the energy spectrum. The theory is validated by means of Direct Numerical Simulations (DNS) of homogeneous, isotropic turbulence using a spectral code, where the trajectories of fluid tracers are computed using several interpolation methods. We show that B-spline interpolation has the best accuracy given the computational cost. Finally, the optimal interpolation order for the different methods is shown as a function of the resolution of the DNS simulation.

I. INTRODUCTION

Pseudo-spectral codes in combination with accurate interpolation methods for particle tracking are commonly used in many applications [1–6]. The spectral code solves the flow field by means of direct numerical simulations in an Eulerian approach, while the particle trajectories are obtained by a Lagrangian approach. To compute the particle trajectories the fluid velocity must be known at the particle positions. The standard way to do this is by representing the Eulerian fluid velocity on a uniform, rectangular grid and make use of appropriate interpolation schemes to evaluate fluid velocities out of the grid. Many interpolation methods have been used, from low-order linear schemes [2] to high-order splines [4–6]. Because the interpolation step is time consuming and memory demanding, it is important to choose the best interpolation method for a given application. In order to get more accurate results the order of the interpolation method can be increased. Because high order methods are computationally expensive, it is important to make the best tradeoff between accuracy and computational costs. The best tradeoff can be determined by using good error estimates, assuring that the high-order methods will give significantly more accurate result.

In many applications, and notably those where almost neutrally buoyant particles are involved, not only the fluid velocity is needed but also its first derivatives. The evaluation of these derivatives can also be computed efficiently by the interpolation method, by taking the derivative of the interpolating function [7]. A good approximation of the first derivative requires accurate interpolation methods. For the computation of the trajectories of (almost neutrally buoyant) particles we consider the equation discussed by Maxey and Riley [8], for small isolated rigid spherical particles ($d_p \ll \eta$, with d_p the particle diameter and η the Kolmogorov length scale) in a non-uniform velocity field $\mathbf{u}(\mathbf{x}, t)$. An important assumption is that the particle Reynolds number is small, $Re_p = d_p|\mathbf{u} - \mathbf{u}_p|/\nu \ll 1$, with $\mathbf{u}_p$ the velocity of the particle and ν the kinematic viscosity of the fluid. Because we consider small particle diameters and small particle volume fractions we ignore the effects of two-way and four-way coupling. An overview of the different terms in the Maxey-Riley (MR) equation and its numerical implementation can be found in the paper by Loth [9] and a historical account of the equation of motion in a review article by Michaelides [10]. Time integration of the MR equation to compute particle trajectories can be an expensive, time- and memory consuming job, particularly for what concerns the computation of the Basset history force. However, a significant reduction in computational costs can be obtained by fitting the diffusive kernel of the Basset history force with exponential functions, as shown by Van Hinsberg *et al.* [11].

A systematic way to determine the best tradeoff between interpolation accuracy and computational cost for a particular application is to compare errors: the interpolation error is compared with the discretisation error of the flow field. In this way one can prevent unnecessary accurate and expensive computations. We will introduce

* Electronic mail: M.A.T.v.Hinsberg@tue.nl
† Electronic mail: H.J.H.Clercx@tue.nl

different practical methods for computing these errors, and will investigate the following interpolation methods: Lagrange interpolation, spline interpolation, Hermite interpolation and B-spline interpolation. For Hermite interpolation we use the method suggested by Choi *et al.* [12] who employed Hermite interpolation on multiple spatial points. For the B-spline interpolation the method of Van Hinsberg *et al.* [7] is used. These methods are also used in many other applications, including the computation of charged particles in a magnetic field [13, 14], but also digital filtering and applications in medical imaging [15, 16]. In the latter case interpolations are used to improve image resolution. Besides the optimization of interpolation algorithms (accuracy, efficiency), the impact of different interpolation methods on physical phenomena, like particle transport, has been investigated in many studies [12, 17–22]. To our knowledge the direct comparison between the interpolation and the discretisation error to make an optimal choise for the interpolation method has not yet been systematized; here we will give fundamental insight into this problem.

The manuscript is arranged as follows. Sections II and III give practical methods on how to estimate the interpolation error. Section II focuses on calculating the interpolation error off-line. In this way only statistics of the turbulent flow are needed without having to compute interpolations. In Section III an even more practical method is proposed. This method only needs the energy spectrum to predict the interpolation error. A practical method for estimating the discretisation error is discussed in Section IV. Next, the different interpolation methods employed are explained in Section V. Thereafter, the results of a comparison are shown in Section VI, where we give a prediction of the optimal order of the interpolation methods provided the spatial resolution of the smallest (turbulent) flow scale is known. Finally, concluding remarks are given in Section VII.

II. INTERPOLATION ERROR

This section focuses on the a-priori estimation of the interpolation error. In this way only the statistics of the turbulent flow is needed without having to compute interpolations, an efficient method for estimating the interpolation error.

In general the particle will follow a path $\mathbf{x}_p(t)$ and the flow velocity field is given by $\mathbf{u}(\mathbf{x},t)$. Suppose that we need to find the velocity at the particle position, i.e., $\mathbf{u}(\mathbf{x}_p(t),t)$, but instead we find the approximation $\widetilde{\mathbf{u}}(\mathbf{x}_p(t),t)$, due to the interpolation errors. Let $\mathcal{I}$ be the interpolation operator that maps $\mathbf{u}$ onto $\widetilde{\mathbf{u}}$, so $\widetilde{\mathbf{u}} = \mathcal{I}[\mathbf{u}]$. The relative interpolation error ϵ for one particle can be computed by the L^2-norm like

$$\epsilon = \lim_{T\to\infty} \frac{\|\mathbf{u}(\mathbf{x}_p(t),t) - \widetilde{\mathbf{u}}(\mathbf{x}_p(t),t)\|_T}{\|\mathbf{u}(\mathbf{x}_p(t),t)\|_T}, \qquad (1)$$

where the time averaging norm, $\|\cdot\|_T^2$ is given by

$$\|\mathbf{f}\|_T^2 = \frac{1}{T}\int_0^T |\mathbf{f}(t)|^2 \mathrm{d}t, \qquad (2)$$

and $|\cdot|$ denotes the usual 2-norm. Analogous to this, the norm is also used for scalar quantities. The value of $\mathbf{u}(\mathbf{x}_p(t),t)$ in relation (1) can be calculated from the Fourier components of the Eulerian flow field (obtained from the DNS), which is computationally expensive. Therefore, relation (1) will only be used to validate the following steps towards a more pragmatic approach to estimate the interpolation error.

We assume that the system is ergodic which means that the ensemble average is equal to the time average, therefore ϵ does not depend on the choice of the particle and an average over particles can be taken. Furthermore, we assume that the particle has no preferential location and thus we can replace the particle average by a space average. We can thus average over space and time, in practice the time average needs to be performed over several large-eddy turnover times. The space average is taken over the whole domain V which is $[0,1)^3$ in dimensionless units. Notice that in order to simplify the notation we have chosen $[0,1)^3$ instead of the usual $[0,2\pi)^3$. In this way one can write ϵ like

$$\epsilon = \frac{\left\| \|\mathbf{u} - \widetilde{\mathbf{u}}\|_3 \right\|_T}{\left\| \|\mathbf{u}\|_3 \right\|_T}, \qquad (3)$$

where we introduce the following inner products

$$\begin{aligned}\langle \mathbf{f}, \mathbf{g}\rangle_1 &= \int_0^1 \left(\mathbf{f}\cdot\mathbf{g}^*\right)(x)\mathrm{d}x,\\ \langle \mathbf{f}, \mathbf{g}\rangle_3 &= \int_0^1\int_0^1\int_0^1 \left(\mathbf{f}\cdot\mathbf{g}^*\right)(\mathbf{x})\mathrm{d}x\mathrm{d}y\mathrm{d}z,\end{aligned} \qquad (4)$$

and the corresponding norms:

$$\begin{aligned}\|\mathbf{f}\|_1^2 &= \langle \mathbf{f}, \mathbf{f}\,\rangle_1 = \int_0^1 |\mathbf{f}(x)|^2 \mathrm{d}x\ ,\\ \|\mathbf{f}\|_3^2 &= \langle \mathbf{f}, \mathbf{f}\,\rangle_3 = \int_0^1\int_0^1\int_0^1 |\mathbf{f}(\mathbf{x})|^2 \mathrm{d}x\mathrm{d}y\mathrm{d}z.\end{aligned} \qquad (5)$$

Here $\mathbf{f}\cdot\mathbf{g}$ denotes the usual inner product and $\mathbf{g}^*$ denotes the complex conjugate of $\mathbf{g}$. These inner products and norms are also used for scalar fields like f and g where the inner product is reduced to the ordinary product fg^*. The velocity field is approximated in a three-dimensional Fourier series, like

$$\mathbf{u}(\mathbf{x},t) = \sum_{\mathbf{k}\in\mathbf{K}} \mathbf{u}_\mathbf{k}(t)\phi_\mathbf{k}(\mathbf{x}), \qquad \phi_\mathbf{k}(\mathbf{x}) = e^{2\pi \mathrm{i}\mathbf{k}\cdot\mathbf{x}}, \quad (6)$$

where $\mathbf{K}$ is the space of wave vectors $\mathbf{k}$, with $\mathbf{k} = (k_x, k_y, k_z)$ and $|\mathbf{k}| \leq k_{\max}$ the maximal wave number. We neglect the error made by taking a finite sum, which is a part of the discretisation error (and should for a well-resolved simulation decrease exponentially in case of increasing resolution). The complex valued functions

$\phi_{\mathbf{k}}$ constitute an orthonormal basis with respect to the inner product $\langle\cdot,\cdot\rangle_3$. Introducing the interpolant of $\phi_{\mathbf{k}}$; $\widetilde{\phi}_{\mathbf{k}} = \mathcal{I}[\phi_{\mathbf{k}}]$, when the interpolation operator $\mathcal{I}$ is linear, one obtains:

$$\epsilon = \frac{\left\| \left\| \sum_{\mathbf{k}\in\mathbf{K}} \mathbf{u}_{\mathbf{k}} \left(\phi_{\mathbf{k}} - \widetilde{\phi}_{\mathbf{k}} \right) \right\|_3 \right\|_T}{\left\| \left\| \sum_{\mathbf{k}\in\mathbf{K}} \mathbf{u}_{\mathbf{k}} \phi_{\mathbf{k}} \right\|_3 \right\|_T}. \tag{7}$$

It can be proven, see [7], that $\phi_{\mathbf{k}} - \widetilde{\phi}_{\mathbf{k}}$ constitute an orthogonal basis with respect to the inner product $\langle\cdot,\cdot\rangle_3$ and we define $\gamma_{\mathbf{k}} = \|\phi_{\mathbf{k}} - \widetilde{\phi}_{\mathbf{k}}\|_3$. In this case we obtain

$$\epsilon = \frac{\left\| \left(\sum_{\mathbf{k}\in\mathbf{K}} \gamma_{\mathbf{k}}^2 |\mathbf{u}_{\mathbf{k}}|^2 \right)^{1/2} \right\|_T}{\left\| \left(\sum_{\mathbf{k}\in\mathbf{K}} |\mathbf{u}_{\mathbf{k}}|^2 \right)^{1/2} \right\|_T} . \tag{8}$$

Changing the order of the norms gives

$$\epsilon = \frac{\left(\sum_{\mathbf{k}\in\mathbf{K}} \gamma_{\mathbf{k}}^2 \left\| \mathbf{u}_{\mathbf{k}} \right\|_T^2 \right)^{1/2}}{\left(\sum_{\mathbf{k}\in\mathbf{K}} \left\| \mathbf{u}_{\mathbf{k}} \right\|_T^2 \right)^{1/2}} . \tag{9}$$

Now ϵ can be calculated without having to do a simulation for all the interpolation methods, only $\|\mathbf{u}_{\mathbf{k}}\|_T$ is needed from the simulations. Next, we require $\mathcal{I}$ to satisfy:

$$\begin{aligned} \tilde{\phi}_{\mathbf{k}} = \mathcal{I}[\phi_{\mathbf{k}}] = \mathcal{I}[\phi_{k_x}\phi_{k_y}\phi_{k_z}] \\ = \mathcal{I}_1[\phi_{k_x}]\mathcal{I}_1[\phi_{k_y}]\mathcal{I}_1[\phi_{k_z}] = \tilde{\phi}_{k_x}\tilde{\phi}_{k_y}\tilde{\phi}_{k_z}, \end{aligned} \tag{10}$$

with $\mathcal{I}_1[\cdot]$ the one-dimensional variant of the operator $\mathcal{I}[\cdot]$. Using this property and $\|\phi_k\|_1 = 1$, $\gamma_{\mathbf{k}}^2$ can be written as

$$\gamma_{\mathbf{k}}^2 = 1 + s_1(k_x)s_1(k_y)s_1(k_z) - 2s_2(k_x)s_2(k_y)s_2(k_z), \tag{11}$$

with

$$s_1(k) = \left\| \widetilde{\phi}_k \right\|_1^2, \qquad s_2(k) = \mathcal{R}\left(\left\langle \widetilde{\phi}_k, \phi_k \right\rangle_1 \right), \tag{12}$$

with $\mathcal{R}(f)$ denoting the real part of f. Here, s_1 and s_2 can be calculated fast using methods from Van Hinsberg *et al.* [7]. Now combining (9) with (11) and (12) gives us a method for the calculation of the interpolation error.

This method is based on the assumptions that there is no preferential position for the particles, an approach that is correct for fluid tracers in incompressible flows. Inertial particles will instead cluster depending on their size and density. The advantage of this method over using relation (1) is that no simulations of particle trajectories in turbulence have to be done when $\|\mathbf{u}_{\mathbf{k}}\|_T$ is known; the statistical information on the turbulent flow field itself is sufficient.

III. APPROXIMATION OF THE INTERPOLATION ERROR

In this section the error estimate ϵ is further simplified. In Eqn (9) a summation must be taken over all three-dimensional vectors $\mathbf{k} \in \mathbf{K}$. In order to evaluate only a one-dimensional sum one can use the assumption of statistical isotropy of the turbulent flow. In the end this results in a practical method that only needs the energy spectrum to predict the interpolation error.

Starting from Eqn (9), the summation is split as:

$$\epsilon^2 = \frac{\sum_{k=0}^{k_{\max}} \sum_{\mathbf{k}\in\mathbf{K}_k} \gamma_{\mathbf{k}}^2 \left\| \mathbf{u}_{\mathbf{k}} \right\|_T^2}{\sum_{k=0}^{k_{\max}} \sum_{\mathbf{k}\in\mathbf{K}_k} \left\| \mathbf{u}_{\mathbf{k}} \right\|_T^2}, \tag{13}$$

where $\mathbf{K}_k$ is a subset of $\mathbf{K}$ which include $\mathbf{k}$ with $k - \frac{1}{2} \leq |\mathbf{k}| < k + \frac{1}{2}$. Next, the approximation is made that $\mathbf{K}_k$ includes $4\pi k^2$ wave vectors (the surface of a sphere with radius k). Assuming statistical isotropy the three-dimensional energy spectrum is spherically symmetric, and we can write $\|\mathbf{u}_{\mathbf{k}}\|_T = \|u_k\|_T$ for $k = |\mathbf{k}|$. Using both assumptions (13) can be approximated with

$$\epsilon_{\text{iso}}^2 = \frac{\sum_{k=0}^{k_{\max}} k^2 \gamma_k^2 \left\| u_k \right\|_T^2}{\sum_{k=0}^{k_{\max}} k^2 \left\| u_k \right\|_T^2}, \qquad \gamma_k^2 = [\gamma_{\mathbf{k}}^2]_{|\mathbf{k}|=k} , \tag{14}$$

where $[\cdot]_{|\mathbf{k}|=k}$ denotes the space average over the surface of a sphere in k-space with radius k. Note that $(k\|\mathbf{u}_k\|_T)^2$ is proportional to the energy of the modes with $k = |\mathbf{k}|$. In this way the integrated energy spectrum in combination with γ_k is sufficient to calculate the error.

In order to be able to compute $[\gamma_{\mathbf{k}}^2]_{|\mathbf{k}|=k}$ easily, the following derivation is made. Starting from $\gamma_{\mathbf{k}} = \|\phi_{\mathbf{k}} - \widetilde{\phi}_{\mathbf{k}}\|_3$ and introducing $e_k = \phi_k - \widetilde{\phi}_k$ one finds:

$$\begin{aligned} \gamma_{\mathbf{k}}^2 = \|\phi_{k_x}\phi_{k_y}\phi_{k_z} - \\ (\phi_{k_x} - e_{k_x})(\phi_{k_y} - e_{k_y})(\phi_{k_z} - e_{k_z})\|_3^2. \end{aligned} \tag{15}$$

We assume that the error is relatively small compared to the actual Fourier component. Under this assumption we have that $\|e_k\|_1 \ll \|\phi_k\|_1 = 1$ and only the lowest powers of e_k need to be taken into account. Using that $\|\phi_k\|_1 = 1$ one obtains:

$$\begin{aligned} \gamma_{\mathbf{k}}^2 &\approx \|e_{k_x}\phi_{k_y}\phi_{k_z} + \phi_{k_x}e_{k_y}\phi_{k_z} + \phi_{k_x}\phi_{k_y}e_{k_z}\|_3^2 \\ &\approx \|e_{k_x}\|_1^2 + \|e_{k_y}\|_1^2 + \|e_{k_z}\|_1^2. \end{aligned} \tag{16}$$

In the last step we neglected the cross terms. We checked that the final contribution of the cross terms in the summation in relation (14) is only of the order of 5 percent, this is due to the fact that these terms mainly average out as they can be both positive and negative.

We restrict ourselves to polynomial interpolations and we define the order n of the method as follows: n is the highest degree of a polynomial for which the interpolation is still exact. When the order of the interpolation method is known the following approximation can be made

$$\|e_k\|_1^2 \approx c k^{2(n+1)}, \tag{17}$$

where c is some constant. The reason for this formula is the following. Given that a method has order n the amplitude of e_k is proportional to the $(n+1)$-th derivative of ϕ_k. From this, one gets that e_k is proportional to k^{n+1}.

(This is also shown by Figure 1 in Section VI.) Using this one finds that

$$\gamma_{\mathbf{k}}^2 \approx ck_x^{2(n+1)} + ck_y^{2(n+1)} + ck_z^{2(n+1)}. \quad (18)$$

Next, the average needs to be taken over a spherical surface, $[\gamma_{\mathbf{k}}^2]_{|\mathbf{k}|=k}$. Because of symmetry reasons we only need to calculate the contribution of $ck_z^{2(n+1)}$, the contributions of the other terms are equal to this one. The calculation for the surface average is done in spherical coordinates $\mathbf{k} = k(\sin\varphi\cos\theta, \sin\varphi\sin\theta, \cos\varphi)$ as follows,

$$\begin{aligned}\frac{1}{3}[\gamma_{\mathbf{k}}^2]_{|\mathbf{k}|=k} &\approx c[k_z^{2(n+1)}]_{k=|\mathbf{k}|} \\ = \frac{c}{4\pi k^2}\int_0^{\pi}\int_0^{2\pi}(k\cos\varphi)^{2(n+1)}k^2\sin\varphi \mathrm{d}\theta\mathrm{d}\varphi \\ = \frac{ck^{2(n+1)}}{4\pi}\int_0^{\pi}\int_0^{2\pi}\cos^{2(n+1)}\varphi\sin\varphi\mathrm{d}\theta\mathrm{d}\varphi \\ = \frac{ck^{2(n+1)}}{2n+3}. \quad (19)\end{aligned}$$

Thus we obtain:

$$\gamma_k^2 = [\gamma_{\mathbf{k}}^2]_{|\mathbf{k}|=k} \approx \frac{3}{2n+3}ck^{2(n+1)} \approx \frac{3}{2n+3}\|e_k\|_1^2. \quad (20)$$

Combining Eq. (14) with (20) results in a practical method that only needs the energy spectrum to predict the interpolation error. Note that some approximations as discussed are needed and therefore the result will be somewhat less accurate than the expression derived in the previous section.

IV. DISCRETISATION ERROR

As we will compare the interpolation error with the Eulerian discretisation error $\bar{\delta}$, we take the same norm for both of them. A first suggestion would be

$$\bar{\delta} = \frac{\left\| \|\mathbf{u} - \widehat{\mathbf{u}}\|_3 \right\|_T}{\left\| \|\widehat{\mathbf{u}}\|_3 \right\|_T}, \quad (21)$$

where $\widehat{\mathbf{u}}$ is the exact Eulerian velocity field. In practice what we call the "exact" velocity field is obtained by using double grid resolution. Expanding $\mathbf{u}$ and $\widehat{\mathbf{u}}$ in a Fourier series gives

$$\bar{\delta} = \frac{\left\| \left\|\sum_{\mathbf{k}\in\mathbf{K}} \mathbf{u}_{\mathbf{k}}\phi_{\mathbf{k}} - \widehat{\mathbf{u}}_{\mathbf{k}}\phi_{\mathbf{k}}\right\|_3 \right\|_T}{\left\| \left\|\sum_{\mathbf{k}\in\mathbf{K}} \widehat{\mathbf{u}}_{\mathbf{k}}\phi_{\mathbf{k}}\right\|_3 \right\|_T}. \quad (22)$$

Due to turbulence the error will grow in time and eventually will become of the same order as the velocity field itself. To avoid this complication we will only look at statistical properties. We take the time average of the Fourier components before comparing the two velocity fields. The new discretisation error δ is therefore defined as:

$$\delta = \frac{\left(\sum_{\mathbf{k}\in\mathbf{K}}\left(\|\mathbf{u}_{\mathbf{k}}\|_T - \|\widehat{\mathbf{u}}_{\mathbf{k}}\|_T\right)^2\right)^{1/2}}{\left(\sum_{\mathbf{k}\in\mathbf{K}}\left\|\widehat{\mathbf{u}}_{\mathbf{k}}\right\|_T^2\right)^{1/2}}. \quad (23)$$

Note that this error is taken in the same way as the interpolation error, see relation (9). Next we use the fact that the energy spectrum for homogeneous isotropic turbulence is spherically symmetric like done before, which results in:

$$\delta_{\mathrm{iso}}^2 = \frac{\sum_{k=0}^{k_{\max}} k^2\left|\|\mathbf{u}_k\|_T - \|\widehat{\mathbf{u}}_k\|_T\right|^2}{\sum_{k=0}^{k_{\max}} k^2\left\|\widehat{\mathbf{u}}_k\right\|_T^2}. \quad (24)$$

This relation can be used to estimate the discretisation error by the use of the energy spectrum.

V. INTERPOLATION METHODS

The theory presented is tested on several different interpolation methods, namely Lagrange interpolation, spline interpolation, Hermite interpolation and B-spline interpolation. In each spatial direction the methods investigated use N data points to construct a polynomial function of degree $N-1$ for the interpolation. For Hermite interpolation we use the method suggested by Choi *et al.* [12] who employ Hermite interpolation on multiple spatial points. For the B-spline interpolation the method of Van Hinsberg *et al.* [7] is used.

In Table I all methods are listed with an overview of their main features. The order of continuity refers to the continuity C^n of the interpolation function. Furthermore with FFT we refer to the number of Fast Fourier Transforms required for the interpolation. For Hermite interpolation also the derivatives are needed and this requirement increases the number of FFTs needed. In Figure 1, $\gamma_k(k\Delta x)$, as from equation (20) is shown for the different interpolation methods, where Δx is the distance between the grid points.

interpolation method	n	order of continuity	FFT	comment
Lagrange	$N-1$	0	1	for even N
		-1	1	for odd N
spline	$N-2$	$(N-2)/2$	1	only even N
Hermite	$N-1$	1	8	only for $N \in 4\mathbb{N}$
B-spline	$N-1$	$N-2$	1	all N

TABLE I. Overview of the interpolation methods considered in this study. Note that for all methods the degree of the polynomial function is equal to $N-1$. n is the highest order of a polynomial function for which the interpolation is still exact[7].

VI. RESULTS

In this section we compare the interpolation methods. The discretisation error is computed and compared with the interpolation error for all the interpolation methods. We estimate the errors by using the methods given by

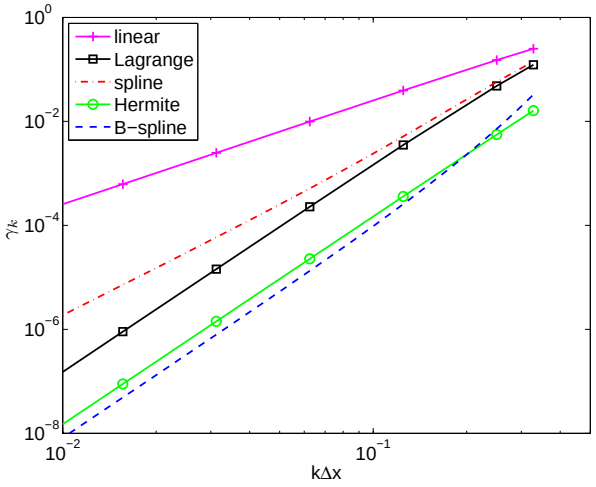

FIG. 1. Interpolation error γ_k (20) of the various methods, calculated with the methods of Van Hinsberg *et al.* [7]. For all methods $N = 4$ except for linear interpolation which has $N = 2$.

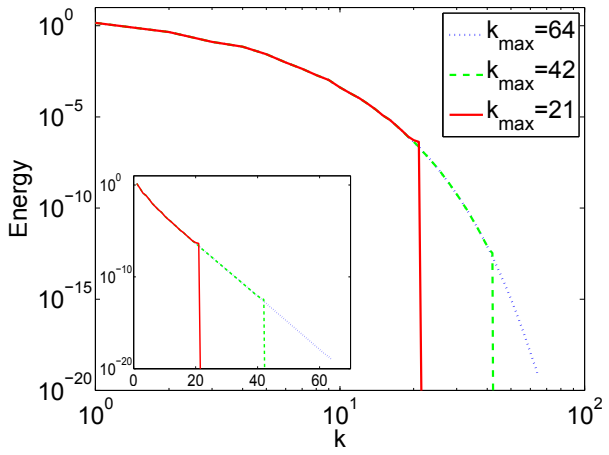

FIG. 2. Energy spectra for different $k_{\max}$ in log-log scale. In the inset the same but in log-lin scale.

Eq. (24), for the discretisation error and by Eq. (14) and (20) for the interpolation error. Subsequently, the methods are validated by investigating two different aspects: the error made in the location of the particles and the acceleration spectrum. Thanks to this quantitative comparison we are able to give a prediction of the optimal order N for the different interpolation methods as a function of $k_{\max}\eta$. Here η is the Kolmogorov length scale.

To compute the discretisation error several simulations of homogeneous isotropic turbulence are performed with different $k_{\max}$, for details see Table II. The energy spectra are reported in Figure 2. Using relation (24) the

grid	number of grid points	$k_{\max}$	ν	$k_{\max}\eta$
coarse	64	21	0.048	2.4
fine	128	42	0.048	4.8
reference	128	64	0.048	7.2

TABLE II. Details of the DNS simulations of homogenous isotropic turbulence. Three grids are used for comparison, a coarse, a fine and a very well resolved (reference) grid.

discretisation error can be computed. Next, also the interpolation error can be computed by directly using relation (1) or the approximate relations (14) and (20). Table III shows the interpolation error, calculated in the two different ways, to check the reliability of the approximation. The two proposed methods are found to be in agreement within 10-20%, while the interpolation error changes over orders of magnitude for the different interpolation methods. The differences between the ways of estimating the interpolation error can be explained by statistical errors and approximations made in the theoretically derived error estimates.

method	N	ϵ (1)	ϵ_{iso} (14) and (20)
linear	2	$5.44 \cdot 10^{-3}$	$4.52 \cdot 10^{-3}$
Lagrange	4	$3.67 \cdot 10^{-4}$	$3.45 \cdot 10^{-4}$
Spline	4	$4.39 \cdot 10^{-4}$	$4.73 \cdot 10^{-4}$
B-spline	4	$3.59 \cdot 10^{-5}$	$3.99 \cdot 10^{-5}$
Hermite	4	$3.82 \cdot 10^{-5}$	$3.13 \cdot 10^{-5}$

TABLE III. Interpolation error for different methods calculated in different ways. Here $k_{\max}\eta = 2.4$ and $\delta = 5.03 \cdot 10^{-4}$.

Next, to check the theory and the influence of the interpolation error, both errors in particle position and acceleration statistics are investigated. We start with the error in the position of the particle. The procedure is as follows: first a family of tracers starting at one point is simulated with different interpolation methods, second the reference tracer is simulated in a second simulation with double grid resolution keeping the initial condition and forcing the same. We started averaging over 50 particles, and in order to check statistical convergence and the eventual dependence on the initial condition, we repeated this for 4 different realizations of the flow field. After checking that the trend is the same the results shown here are averaged over the 4 realizations, for a total of 200 particles. The error in the particle position is plotted in Figure 3 using different norms,

$$L^M = \|\mathbf{x}_p - \widetilde{\mathbf{x}}_p\|_M, \qquad \|\mathbf{f}\|_M = \left(\sum_p |\mathbf{f}_p|^M \right)^{\frac{1}{M}}, \quad (25)$$

where $\widetilde{\mathbf{x}}_p$ is the particle trajectory calculated by using interpolation methods and $\mathbf{x}_p$ is the exact particle trajectory, calculated using double grid resolution. In Figure 3 one can see that even after one large eddy turnover time, t=1, the influence of the interpolation error dominates over chaotic behavior of turbulence. At t=1 the errors for the different methods are still clearly separated.

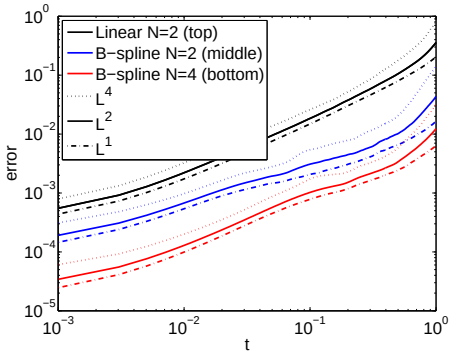

FIG. 3. The error in the position of tracers for different interpolation methods and using different norms. The errors are plotted as a function of time and averaged over multiple particles.

Next, we consider the L^2-error after the Kolmogorov time scale ($t = 0.15$) for the different interpolation methods, see Figure 4. In the following we focus on the L^2-norm because this is the norm used in Sections II and III. In

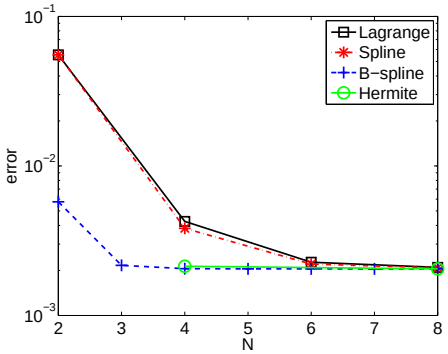

FIG. 4. L^2-error at the position of a tracer after the Kolmogorov time scale ($t = 0.15$), with $k_{\max}\eta = 2.4$. The error is a combination of the interpolation and discretisation error.

Figure 4 one can see that higher order interpolations indeed become more accurate and that for high N no further accuracy is gained because the discretisation error has become dominant over the interpolation error. This behavior is in agreement with the results in Table III. When increasing the resolution the discretisation error becomes smaller and higher order interpolation methods are needed to maintain the accuracy after interpolation, see Figure 5.

In order to better show the influence of interpolation methods we investigate the acceleration of the particle. Not only is the acceleration itself of great interest as a statistical quantity, see for example Ref. [1], but it is also needed to calculate the hydrodynamic forces in the Maxey-Riley equation. The acceleration signal of a generic particle as a function of time is shown in Figure 6. The high frequency oscillations are clearly nonphysical and with more accurate interpolation methods they

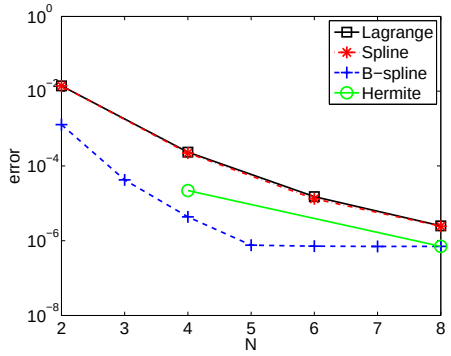

FIG. 5. L^2-error at the position of a tracer after the Kolmogorov time scale, with $k_{\max}\eta = 4.8$. The error is a combination of the interpolation and discretisation error.

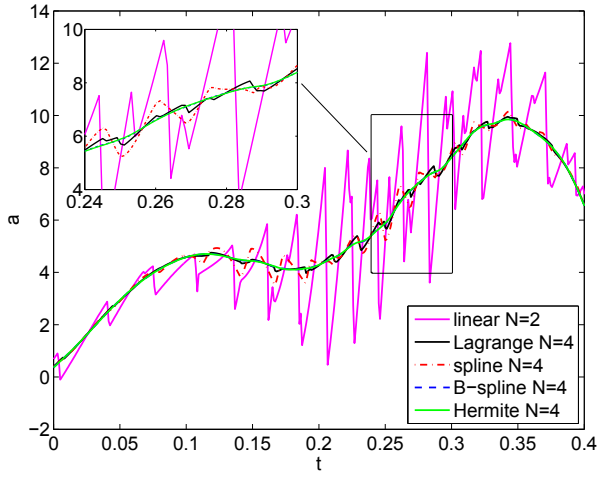

FIG. 6. Particle acceleration of a fluid tracer, computed with different interpolation methods, where $k_{\max}\eta = 2.4$. The zigzagging is an artifact of the interpolation method.

disappear. To better quantify this effect we analyze the acceleration spectrum of the particles. From Figure 7 it

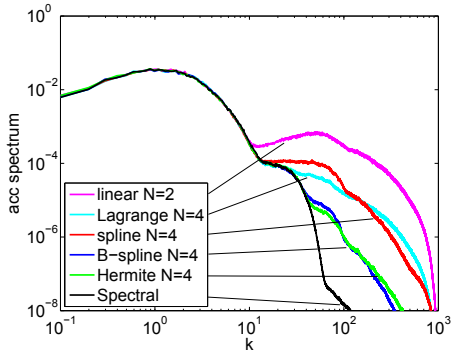

FIG. 7. Particle acceleration spectrum, with $k_{\max}\eta = 2.4$. On the right side artificial energy is added due to both the interpolation and discretisation error.

can be seen that even the spectral interpolation shows

a kink in the spectrum (around $k = 13$) due to the discretisation error. For higher $k_{\max}\eta$ this kink is still observed but at higher wave numbers. The energy content within the range of wavenumbers between 20 and 3000 is computed and used as an error indication, see Figure 8. Again the same behavior is found as in Figures 4 and 5,

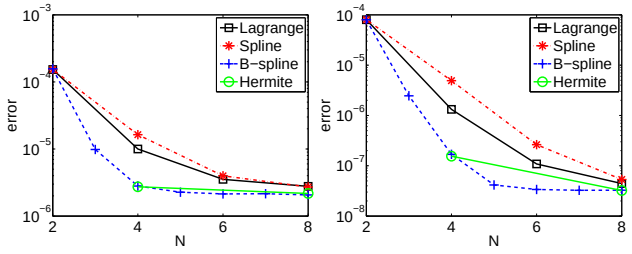

FIG. 8. The error in the acceleration spectrum is plotted as a function of N, the order of the interpolation function. As error indication we employ the energy contained in the particle acceleration spectrum between wavenumbers 20 and 3000. The error is a combination of both the interpolation and discretisation error. (left panel) $k_{\max}\eta = 2.4$ (right panel) $k_{\max}\eta = 4.8$

as predicted by the theory.

Now that the methods are validated for computing the interpolation error, the theory can be used to forecast which interpolation method is optimal for a given $k_{\max}\eta$. As increasing N of the interpolation method is much less time consuming than improving the resolution, the interpolation error is not allowed to exceed the discretisation error. Using this criterium the optimal N can be found for a given $k_{\max}\eta$ and interpolation method, see Figure 9. In this simulation we did not allow for any aliasing of

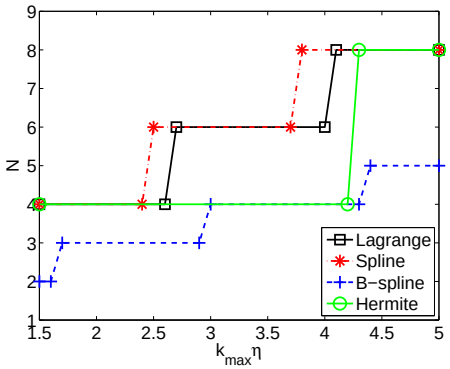

FIG. 9. Optimal order N for the different interpolation methods with $k_{\max} = \frac{1}{3\Delta x}$. The optimal N is found by the criterium that the interpolation error is not allowed to exceed the discretisation error.

the nonlinear term, therefore $k_{\max} = \frac{1}{3\Delta x}$. In order to increase the accuracy, $k_{\max}$ can be increased allowing for some aliasing, see Figure 10.

From Figures 9 and 10 it can be seen that interpolation methods become more important when going to higher values of $k_{\max}\eta$. Typical $k_{\max}\eta$ values used are

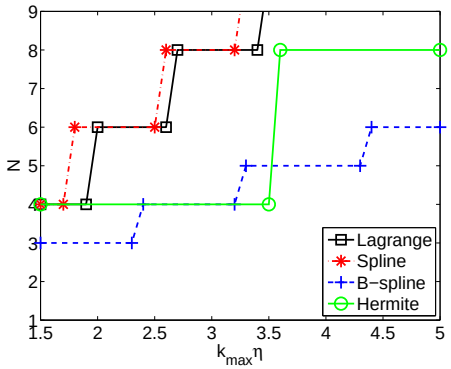

FIG. 10. Optimal order N for the different interpolation methods, with $k_{\max} = \frac{\sqrt{2}}{3\Delta x}$. The optimal N is found by the criterium that the interpolation error is not allowed to exceed the discretisation error.

around 1.5 but studies have been performed with values up to 34 [23]. As the full Maxey-Riley equation also use derivatives of the flow field the accuracy of the flow field should be increased, implying $k_{\max}\eta \approx 3$ or higher. Here, B-spline interpolation is by far outperforming the other interpolation methods. The only interpolation method that is comparable is the Hermite interpolation, however a drawback is that it can only be used for N a multiple of 4, thus limiting its flexibility. Furthermore, in order to employ Hermite interpolation also derivatives are needed making it computationally expensive (due to the need to evaluate many FFTs per derivative). To conclude, we found that B-spline interpolation is very suited for particle tracking simulations.

VII. CONCLUSIONS

We have introduced different practical methods for computing the error in the interpolation of the fluid velocity. First, we have introduced an accurate method that uses the full three-dimensional energy spectrum to estimate this error. Second, we introduced a practical method that only needs the one-dimensional energy spectrum to estimate the same error. These methods are validated by means of turbulent simulations and it is shown that they give accurate results.

Further we show the effect of the interpolation methods on both errors of particle positions and the acceleration spectrum. Particularly the latter is important because the particle acceleration enters directly in the Maxey-Riley equation. The results for both the errors on particle positions and the acceleration spectrum are in agreement with the predictions of the theory.

Finally, we could provide a prediction for the optimal order of the different interpolation methods as a function of $k_{\max}\eta$. In order to investigate the behavior of almost neutrally buoyant particles also derivatives of the flow field need to be accurately resolved, this implying

values of $k_{\max}\eta$ around 3 or higher. At these values of $k_{\max}\eta$, B-spline interpolation performs much better than the other interpolation methods, implying less computational overhead.

VIII. ACKNOWLEDGEMENTS

We thank B.J.H. van de Wiel for fruitful discussions. The authors gratefully acknowledge financial support from the Dutch Foundation for Fundamental Research on Matter (FOM) (Program 112 "Droplets in Turbulent Flow"). This work was sponsored by the Stichting Nationale Computerfaciliteiten (NCF) for the use of supercomputer facilities, with financial support from the Netherlands Organization for Scientific Research (NWO). The European COST Action MP0806 "Particles in Turbulence" is also acknowledged.

[1] F. Toschi and E. Bodenschatz. Lagrangian properties of particles in turbulence. *Annu. Rev. Fluid Mech.*, **41**:375–404, 2009.

[2] L. Biferale, G. Boffetta, A. Celani, B.J. Devenish, A. Lanottea, and F. Toschi. Lagrangian statistics of particle pairs in homogeneous isotropic turbulence. *Phys. Fluids*, **17**:115101, 2005.

[3] E. Calzavarini, R. Volk, E. Lévêque, J.-F. Pinton, and F. Toschi. Impact of trailing wake drag on the statistical properties and dynamics of finite-sized particle in turbulence. *Physica D*, **241(3)**:237–244, 2012.

[4] R. Benzi, L. Biferale, R. Fisher, D.Q. Lamb, and F. Toschi. Inertial range Eulerian and lagrangian statistics from numerical simulations of isotropic turbulence. *J. Fluid Mech.*, **653**:221–244, 2010.

[5] F. Lekien and J. Marsden. Tricubic interpolation in three dimensions. *Int. J. Numer. Meth. Engng*, **63**:455–471, 2005.

[6] E. Catmull and R. Rom. A class of local interpolating splines. In Computer Aided Geometric Design, editor, *R. E. Barnhill and R. F. Reisenfeld*, pages 317–326. Eds. Academic Press, New York, 1974.

[7] M.A.T. van Hinsberg, J.H.M. ten Thije Boonkkamp, F. Toschi, and H.J.H Clercx. On the efficiency and accuracy of interpolation methods for spectral codes. *SIAM J. Sci. Comput.*, **34(4)**:B479–B498, 2012.

[8] M.R. Maxey and J.J. Riley. Equation of motion for a small rigid sphere in a nonuniform flow. *Phys. Fluids*, **26**:883–889, 1983.

[9] E. Loth. Numerical approaches for motion of dispersed particles, droplets and bubbles. *Prog. Energ. Combust.*, **26**:161–223, 2000.

[10] E.E. Michaelides. Hydrodynamic Force and Heat/Mass Transfer From Particles, Bubbles, and DropsThe Freeman Scholar Lecture. *J. Fluids Eng.*, **125(2)**:209–238, 2003.

[11] M.A.T. van Hinsberg, J.H.M. ten Thije Boonkkamp, and H.J.H Clercx. An efficient, second order method for the approximation of the Basset history force. *J. Comput. Phys.*, **230(4)**:1465–1478, 2011.

[12] J. Choi, K. Yeo, and C. Lee. Lagrangian statistics in turbulent channel flow. *Phys. Fluids*, **16**,779, 2004.

[13] G.D. Reeves, R.D. Belian, and T.A. Fritz. Numerical tracking of energetic particle drifts in a model magnetosphere. *J. Geophys. Res.*, **96**:13,997–14,007, 1991.

[14] F. Mackay, R. Marchand, and K. Kabin. Divergence-free magnetic field interpolation and charged particle trajectory integration. *J. Geophys. Res.*, **111**:A06208, 2006.

[15] T.M. Lehmann, C. Gönner, and K. Spitzer. Survey: Interpolation Methods in Medical Image Processing. *IEEE Trans. Med. Imag.*, **18**:1049–1075, 1999.

[16] H.S. Hou and H.C. Andrews. Cubic splines for image interpolation and digital filtering. *IEEE Trans. Acoust., Speech, Signal Processing*, ASSP-**26**, no. **6**:508517, 1978.

[17] H. Homann, J. Dreher, and R. Grauer. Impact of the floating-point precision and interpolation scheme on the results of DNS of turbulence by pseudo-spectral codes. *Comput. Phys. Commun.*, **177**:560–565, 2007.

[18] C. Marchioli, V. Armenio, and A. Soldati. Simple and accurate scheme for fluid velocity interpolation for Eulerian-Lagrangian computation of dispersed flows in 3D curvilinear grids. *Comput. Fluids*, **36**:1187–1198, 2007.

[19] C. Marchioli, A. Soldati, J.G.M. Kuerten, B. Arcen, A. Tanire, G. Goldensoph, K.D. Squires, M.F. Cargnelutti, and L.M. Portela. Statistics of particle dispersion in direct numerical simulations of wall-bounded turbulence: results of an international collaborative benchmark test. *Int. J. Multiphase Flow*, **34**:879893, 2008.

[20] G.B. Jacobs, D.A. Kopriva, and F. Mashayek. Towards efficient tracking of inertial particles with high-order multidomain methods. *J. Comput. Appl. Math.*, **206**:392–408, 2007.

[21] G.E. Karniadakis and J.S. Hesthaven. Spectral interpolation in non-orthogonal domains: algorithms and applications. *J. Eng. Math.*, **56**:201–202, 2006.

[22] C.C. Lalescu, B.Teaca, and D.Carati. Implementation of high order spline interpolations for tracking test particles in discretized fields. *J. Comput. Phys.*, **229**:5862–5869, 2010.

[23] J. Schumacher, K.R. Sreenivasan, and P. K. Yeung. Very fine structures in scalar mixing. *J. Fluid Mech.*, **531**:113–122, 2005.

PREVIOUS PUBLICATIONS IN THIS SERIES:

Number	Author(s)	Title	Month
12-36	L. Gulikers J.H.M. Evers A. Muntean A. Lyulin	The effect of perception anisotropy on particle systems describing pedestrian flows in corridors	Oct. '12
12-37	K. Kumar M. van Helvoort I.S. Pop	Rigorous upscaling of rough boundaries for reactive flows	Oct. '12
12-38	E.J.W. ter Maten R. Pulch W.H.A. Schilders H.H.J.M. Janssen	Efficient calculation of uncertainty quantification	Nov. '12
12-39	C. Kaufmann M. Günther D. Klagges M. Richwin S. Schöps E.J.W. ter Maten	Coupled heat-electromagnetic simulation of inductive charging stations for electric vehicles	Nov. '12
12-40	M.A.T. van Hinsberg J.H.M. ten Thije Boonkkamp F. Toschi H.J.H. Clercx	On optimal interpolation schemes for particle tracking in turbulence	Nov. '12

Ontwerp: de Tantes,
Tobias Baanders, CWI